MISS ROBYN JEAN TIN YU GRAHAM (Orcid ID : 0000-0002-7561-0570)
DR. EUGENIO CILLAN GARCIA (Orcid ID : 0000-0002-8840-4098)
DR. BRUCE BLADON (Orcid ID : 0000-0001-9204-725X)

Article type : General Article

Editorial ref. code: EVJ-GA-18-265.R3

Metabolomic analysis of synovial fluid from Thoroughbred racehorses diagnosed with palmar osteochondral disease using magnetic resonance imaging

R. J. T. Y. Graham*[a], J. R. Anderson[b], M. M. Phelan[c,d], E. Cillan-Garcia[a], B. M. Bladon[e] and S. E. Taylor[a]

[a]Equine Hospital, Royal (Dick) School of Veterinary Studies, University of Edinburgh, Midlothian, EH25 9RG, UK;
[b]Institute of Ageing and Chronic Disease, University of Liverpool, Liverpool, UK;
[c]Institute of Integrative Biology, University of Liverpool, Liverpool, UK;
[d]HLS Technology Directorate, University of Liverpool, Liverpool, UK and
[e]Donnington Grove Veterinary Group, Newbury, Berkshire, RG14 2JB, UK.

*Corresponding author email: robyn.graham@ed.ac.uk

Keywords: horse; metacarpophalangeal joint; palmar osteochondral disease; magnetic resonance imaging; synovial fluid; metabolomics
Running head: Metabolomic analysis of synovial fluid to diagnose palmar osteochondral disease

Summary

Background: Palmar osteochondral disease (POD) is a common cause of lameness in competition horses. Magnetic resonance imaging (MRI) is the most sensitive diagnostic modality currently available, however it may not be financially nor logistically practical for routine screening of POD. There is increasing interest in the use of metabolomics for diagnosis prior to progression to irreversible damage.

Objectives: To determine metabolite levels in synovial fluid (SF) of horses with a clinical diagnosis of POD based on diagnostic analgesia and MRI, with the hypothesis that metabolomic profiles differ between diseased and healthy joints.
Study design: Prospective clinical study.
Methods: Synovial fluid was collected from metacarpo/tarsophalangeal joints (MC/TPJ) of 29 horses (n = 51 joints), including 14 controls (n = 26) and 15 cases (n = 25), the latter with lameness localised to the MC/TPJ and MR changes consistent with POD (n = 23). Spectra were produced using ^{1}H-nuclear magnetic resonance (NMR) spectroscopy and analysed.
Results: Twenty-five metabolites were recognised associated with various biosynthetic and degradation pathways. The metabolite abundances within the controls demonstrated increased variability compared with the clinical group. The low level of variance between the spectra of the two groups was explained by 5 principal components. Cross-validation of the cohort demonstrated modest separation of predictive power (R^2 = 0.67; Q^2 = 0.34). Although statistical significance was not achieved, the most influential metabolites were glucose and lactate.
Main limitations: The modest sample size and variation in signalment, background and presenting condition of the controls may have impacted the discriminative power of the constructed models. The lack of matched controls, differences in time of fluid collection and freezing times may have also reduced accuracy when representing metabolite profiles.
Conclusions: This study identified and quantified metabolites present in MC/TPJ SF of clinical cases with POD.

Introduction

Palmar osteochondral disease (POD) is an important cause of lameness and wastage in competition horses. Lesions have been identified in 55-80.4% of all Thoroughbred (TB) racehorses in at least one metacarpal/metatarsal (MC/T) condyle, with 14% reporting severe disease [1-4]. Subchondral bone (SCB) inflammation in the palmar/plantar apical region of MC/TIII bones occurs due to traumatic injury and chronic overloading in bones repeatedly exposed to fast work. The resultant sclerosis, necrosis and cartilage thinning weakens the bone making it less capable of withstanding stresses associated with training and racing [5]. This eventually leads to focal resorption and formation of a void in the cartilage, followed by collapse of the articular surface, at which point the overlying articular cartilage is no longer viable. Early recognition of the condition is therefore vital to facilitate prompt treatment and/or management changes.

Advanced imaging is required for diagnosis prior to manifestation of irreversible damage, making early identification, monitoring and prognostication a challenge for many ambulatory veterinarians for which access to these imaging modalities may not be readily available. Magnetic resonance imaging (MRI) accurately represents cartilage and SCB density and thickness [6] and has been validated for detection of lesions in the metacarpal/tarsophalangeal joint (MC/TPJ) [2,7-10], however some abnormal MRI findings

consistently recognised with POD are seen in normal horses in training and additional diagnostic methods are therefore required to facilitate early detection.

Metabolomics is a powerful systems biological approach that simultaneously measures all metabolites present within biological fluids or tissues [11]. Metabolite phenotypic profiling captures relationships of the cellular processes they represent. It provides multi-dimensional information on biochemical responses of complex systems to a range of intrinsic and environmental stimuli under specific circumstances [12-14], with the ultimate aim of serving as unique 'fingerprints' or disease biomarkers in named pathological states. Compared with other biochemical techniques, metabolomics requires minimal pre-treatment and processing and has been used successfully in the rapid assessment of numerous systemic disease states in human and veterinary medicine [15-20]. Metabolites within synovial fluid (SF) accurately represent activity of the surrounding synovial tissues, bones and cartilage [14] and recent equine studies report successful differentiation of osteoarthritis [21], osteochondrosis [22] and joint sepsis [20].

The aim of this study was to investigate equine SF metabolomics from samples collected in a clinical environment and to identify potential metabolite biomarkers in cases with MRI-diagnosed POD, with the hypothesis being metabolomic profiles are different between diseased and healthy joints.

Materials and Methods

Clinical cases were recruited from horses presenting to the Royal (Dick) School of Veterinary Studies Equine Hospital for lameness investigation between January 2015 and March 2018 and consisted predominantly of Thoroughbred racehorses in training from one racing yard. Criteria for inclusion were: 1) lameness localised to the MC/TPJ based on regional or intra-articular analgesia; 2) absence of other causative lesions within the joint on comprehensive radiographic examination; 3) MRI changes consistent with those described for POD [2]. Inclusion criteria for control horses were: 1) clinical presentation for unrelated conditions or lameness that did not improve upon intra-articular analgesia of the MC/TPJ; 2) absence of pathology on subsequent MRI of the MC/TPJ. Some of the control cases necessitated euthanasia for humane reasons due to the initial presenting conditions.

Magnetic Resonance Imaging

The MRI scans were obtained under standing sedation using a 0.27-Tesla dedicated and fully calibrated equine MRI system[a]. T1 and T2-weighted gradient echo (GRE) and short tau inversion recovery (STIR) GRE sequences were acquired in transverse, dorsal and sagittal planes. High resolution scans were acquired wherever possible and some sequences used live-motion correction techniques [2]. The scans were blindly reviewed using an open-source DICOM viewer[b] by two equine clinicians, one of whom was experienced in interpretation of low-field MR images (S.E.T). The medial and lateral condyles of the MC/TIII bones were assessed using a POD score adapted from Olive *et al.* [23] and based mainly on T1 and T2-weighted images, with STIR included where available. Briefly, grade 0 described normal SCB, grade 1 mild

sclerosis, grade 2 moderate to marked sclerosis, grade 3 SCB resorption and grade 4 subchondral collapse or fragmentation. The presence of subchondral bone marrow lesions was marked with an asterisk (*). The same sequence of scans was carried out on the distal limbs of control cases. In those requiring euthanasia, scans were performed within 12 hours of death.

Sample collection

Synovial fluid was aspirated from the affected MC/TPJ at the time of intra-articular analgesia or medication or within 10 minutes of euthanasia of those euthanased. One ml of SF was placed into uncoated 1.5 ml collection tubes and the sample centrifuged at 1600 *g* for 5 minutes at room temperature to remove particulate matter prior to transfer of the cell-free supernatant into a clean collection tube. This was snap-frozen using liquid nitrogen and stored at -80°C for a maximum freezing time of 8 months.

Sample preparation

The samples were thawed over ice and 300 µl of SF suspended in a buffer solution containing 50%(v/v) SF, 40%(v/v) deuterium oxide (18.2MΩ), 10%(v/v) 1M sodium phosphate pH 7.4 buffer[d] and 0.0025%(v/v) sodium azide[e]. The samples were vortexed for one minute and centrifuged at 13000 *g* at 4°C for 2 minutes prior to transfer of 590 µL into 5-mm outer diameter NMR tubes.

NMR acquisition and spectra processing

One dimensional (1D) ^{1}H-NMR spectra with Carr-Purcell-Meiboom-Gill (CPMG) filter was acquired using a 700-MHz Bruker Avance-III spectrometer with a TCI cryoprobe and chilled Sample-Jet autosampler. Standard vendor-supplied pulse sequences (noesypr1d and cpmgpr1d) were used for statistical analysis. The spectra were acquired at 36.8°C with a 4-second interscan delay, 32 transients and 15-ppm spectral width using Topsin 3.1 and IconNMR 4.6.7. Results were processed with automated phasing, baseline correction and a standard vendor-processing routine. The spectra were measured in a proton NMR spectroscopy lock mode using deuterium oxide as internal lock. The left signal of the alpha-glucose anomeric doublet was aligned to 5.244 ppm.

Metabolite annotation and identification

The results were evaluated visually and all spectra scrutinised prior to inclusion in statistical analysis to ensure community-recommended quality control criteria were met [24]. This included consistent line-widths, a flat baseline and water suppression to a signal of less than 0.4 ppm wide. Spectra that met the criteria were divided into regions ('buckets') and metabolites annotated from Chenomx NMR 330-mammalian metabolite library. Each bucket was labelled with the metabolite peak identity from the pattern file. Buckets attributed to ethanol were omitted for multivariate analysis. Identities were confirmed by a combination of ^{1}H 1D-NMR and, where possible, in-house two-dimensional (2D) ^{1}H^{13}C Heteronuclear Single Quantum Coherence NMR standards. As not all ^{1}H NMR spectra were acquired at the same time, spectra were assessed for batch effect between runs using iconNMR and MetaboAnalyst.

Data analysis

The spectra were divided into two groups (POD and control) and analysed using MetaboAnalyst 4. The 'bucketed' data was normalised to the median to improve statistical reliability and reduce any systemic bias arising from sampling inconsistencies. Pareto-scaling was carried out for multivariate analysis. Univariate analysis was performed using t-tests with application of a False-Discovery Rate (FDR) adjusted P-value of 0.05. Multivariate analysis included unsupervised Principal Component Analysis (PCA) and Partial Least Squares Discriminant Analysis (PLS-DA) to determine the optimal number of components for the model. Statistical significance was set at $P \leq 0.05$ following correction for multiple testing using the Benjamini-Hochberg FDR method. Quantile and PCA plots were generated by standard analytical routines using the software package 'R'.

Results

A total of 79 MC/TPJ met the inclusion criteria (clinical 30; controls 49) and spectra from 51 samples (29 horses) met quality control criteria (clinical 25; controls 26) (Table 1). The remainder were excluded due to processing inconsistencies resulting in analog-to-digital converter overflow.

Magnetic Resonance Imaging

In total, 20 condyles were graded as grade 1, 14 as grade 2 and 8 as grade 3, with 11 cases demonstrating concurrent bone marrow lesions (Figs 1 and 2). No grade 4 lesions were noted. Three condyles showed no evidence of POD and one condyle demonstrated a fissure fracture. All control joints had a POD score of 0. The results are detailed in Supplementary Item 1.

Metabolomics

The NMR spectra for both groups demonstrated a consistent set of metabolite signals and all signals were well-matched. Following division of the NMR spectral extracts into individual spectral bins accounting for one or more multiplets, 139 metabolite signals were detected in each extract. Of these, 107 (78.7%) were annotated to 48 metabolites and identification confirmed for 25 using an in-house library and reported with their Metabolomics Standards Initiative level [24] (Table 2). Buckets with values missing following processing were randomly distributed across the dataset. The spectra from the sample from the joint with the fissure fracture was analysed separately and although no quantifiable differences were identified, the sample was not included in the general analysis. No batch effect was observed between spectra acquired at different times and thus batch correction was not required.

The metabolite abundances within the POD group demonstrated lower variability compared with the control group. Within the control group, eight samples from non-Thoroughbred cases were set apart from the general cluster however univariate analysis showed the differences in levels of specific metabolites within these samples did not reach statistical significance. Multivariate analysis using unsupervised PCA

demonstrated minimal variance to be present between the spectra of the POD and control groups and statistical significance was not met (Fig 3). Ninety-five percent of this variance was explained by five principal components (PC), with PC1 and PC2 explaining 58.2% of variance. Supervised multivariate discriminate analysis using PLS-DA plots of the known metabolites identified the optimal model comprising two components and demonstrating moderate predictive power (R^2 = 0.67, Q^2 = 0.34) (Fig 4). The most influential metabolites were glucose and lactate, with decreased levels seen in POD cases (Fig 5).

Discussion

This study used metabolomics to analyse SF collected in a clinical setting from horses with POD. Although no significantly differentiating metabolites were identified, reduced concentrations of glucose and lactate were found in clinical cases. Signal alterations of specific metabolites are identified in sclerotic SCB and thought to reflect hypoxic intra-cellular conditions [25]. Cartilage damage induces a local pathologic inflammatory response that perpetuates a cycle of cartilage destruction and progressive joint injury [26]. Additionally, proliferation of inflammatory cells in synovitis will increase the metabolic state within the joint [27]. Upregulation of the glucose transporter GLUT-1 occurs in hypoxic environments [28] and chondrocytes from human patients with osteoarthritis switch from oxidative phosphorylation to anaerobic glycolysis in order to provide energy for proinflammatory pathways [29]. We hypothesise a similar scenario occurs in POD, thereby explaining the reduced glucose levels in SF seen in clinical cases. Reduced levels of lactate were unexpected, as lactate has been previously demonstrated to accumulate in hypoxic environments following conversion of pyruvate into lactate by lactate dehydrogenase in the absence of oxygen [27]. This finding may potentially be related to the fact sampling of controls was performed post-mortem in the majority of cases (Table 1), which may have resulted in the increased lactate levels seen in the controls relative to clinical cases. Although all samples were collected without delay following euthanasia in an attempt to minimise post-mortem changes, the authors acknowledge the potential exists for metabolites to be altered from their normal state due to hypoxia [18]. Consequently, there is a need to undertake future studies including only ante-mortem samples of both cases and controls in order to confirm the significance, if any, of this finding. In addition, although MRI is an accurate representation of cartilage and SCB density [6], gross and histological examination of the condyles would have improved accuracy of grading of disease severity [1,33] however this was not possible given the design of the study.

One main limitation of the study was the low number of samples that produced quantifiable spectra. It is challenging to establish appropriate numbers required for metabolomic studies due to large numbers of variables present. However, all previous equine metabolomics studies have included similarly moderate numbers. The current model has demonstrated that differences exist in signal strength of a number of metabolites between the two groups. Increased variance between groups is expected with larger cohorts and stronger models with greater R^2 and Q^2 values. This larger variance is expected to improve sensitivity in the identification of specific metabolites with differing levels between the two cohorts. One example of

this includes the up-regulation of taurine metabolism, which was demonstrated in sclerotic SCB in a previous study [25].

Compared to other forms of 'omics' technology, NMR spectroscopy requires less sample preparation and can generate a comprehensive metabolic profile from intact biofluids and tissues [30]. It is therefore preferred for analysis of native samples as it may be conducted in subclinical settings with high throughput [31]. Between cohorts of the same breed, low variations are reported in the metabolic phenotypes and metabolic uniformity is seen despite differing ages, environment and fitness levels [11]. Escalona *et al.* [11] hypothesised these findings to be due to the relatively homogenous genetic and environmental backgrounds of the TB breed. This is consistent with previous mammalian studies [32] and evidenced in the current study by the increased variability of metabolite abundances demonstrated between controls compared with the POD group, the latter of which consisted predominantly of TB racehorses from a single yard that were managed in a similar manner. This was another significant limitation of the study, as the difficulty in acquiring an adequate number of breed-matched control cases meant the control group included samples from horses that varied in signalment, background and presenting conditions. As metabolomes are affected not only by disease processes but also other intrinsic and extrinsic influencers, results of future studies would be strengthened significantly by the inclusion of breed-matched controls.

We recognised that freezer-storage time had the potential to affect cell-processing pathways and negatively influence metabolite profiles, hence the reason batch effect was examined in case any significant systemic variations existed in samples stored for different lengths of time prior to processing. However, batch testing revealed the time of spectra acquisition had no impact on the results. In our experience, samples may be stored for up to 12 months without affecting metabolomic profiles, which is similar to the negligible impact that long-term storage at -80°C appears to have on serum samples [34].

Ethanol is a recognised contaminant resulting from surgical disinfectant of the synoviocentesis site [20] and although acknowledged as the end-product of several known metabolic pathways and drug metabolism, in the authors' experience is rarely identified as a native metabolite in mammals and may in fact negatively represent profiles. As a result, the 'buckets' attributed to the ethanol peak were omitted for multivariate analysis.

One-dimensional NMR is the industry standard for statistical analysis however does result in some overlapping of the signals from the metabolites. Two-dimensional NMR, which includes the naturally occurring ^{13}C, separates these signals and is therefore useful for confirmation of the identity of specific metabolites, although the ability to quantify results is reduced. Increased utilisation of 2D-NMR technology and a greater number of in-house standards would therefore improve confidence of metabolite recognition and facilitate identification of the remaining unidentified metabolites. In addition, proteomics should be

considered in future POD SF studies as proteins are more stable and robust and therefore less sensitive to processing inconsistencies.

The use of metabolomics to analyse SF is a relatively novel concept in equine medicine and this study confirmed its applicability in analysis of samples collected in a clinical environment. In addition, the study provides baseline metabolomic information for future research into POD and other similar degenerative joint diseases. Although no metabolite abundances were statistically different between POD and control groups, there were patterns of change in certain metabolites which warrant further investigation to determine if metabolic fingerprints can be identified with higher numbers. Further validation is required with a larger sample set and matched controls obtained under the same circumstances to confirm candidate markers. A panel of biomarkers has more strength to discriminate a disease process than a single metabolite. Establishment of one such panel would improve diagnostic capacity and allow treatment and management changes may be put into place to halt or slow progression of the disease.

Authors' declaration of interests

No competing interests have been declared.

Ethical animal research

The study was approved by the University of Edinburgh Ethics Committee (VERC 46/15).

Owner informed consent

Owner consent was obtained for all samples included.

Sources of funding

This project and R. Graham's clinical scholarship were kindly funded by the Horserace Betting Levy Board.

Acknowledgements

The authors would like to thank the following people for their contributions: the veterinarians and support staff at the R(D)SVS Equine Hospital for their assistance, in particular Linda George, Douglas Callaghan and Carolyne Sheridan for the acquisition of images; Dr Mandy Peffers and Professor Peter Clegg for input into study design and technical advice. In addition, the authors would like to acknowledge the ongoing provision of clinical samples by Lucinda Russell and Peter Scudamore as we work together towards injury prevention in racehorses.

Authorship

S. Taylor, B. Bladon and E. Cillan-Garcia developed the idea for the article and R. Graham contributed to the conception and design. The samples were collected by R. Graham, E. Cillan-Garcia and S. Taylor and processed by R. Graham and J. Anderson. Data analysis and interpretation were performed by R. Graham,

J. Anderson and M. Phelan. The manuscript was prepared by R. Graham and all authors were involved in critical revision and final approval.

Manufacturers' addresses

[a]Hallmarq EQ2, Guildford, Surrey, UK.

[b]Horos Project 2015 (version 3.1)

Tables

Table 1: Further details of clinical and control cases**.**

	CLINICAL CASES	CONTROLS
Number of cases	15 horses (14 TB)	14 horses (10 TB)
Median age (range)	7 (4-10)	TB 7 (4-20) Others 5 (5-15)
Number of samples	25	26
Limbs involved	LF 2 RF 3 LF RF 14 RH 6	LF 3 RF 1 LF RF 20 RH 2
Time of synoviocentesis	AM 25	AM 8 PM 18

TB = Thoroughbred; LF = left fore; RF = right fore; RH = right hind; AM = ante-mortem; PM = post-mortem

Table 2: Metabolites identified and annotated by Chenomx.

Database identifier	Metabolite Identification	Reliability
HMDB00357	3-Hydroxybutyrate	MS Level 2
HMDB01149	5-Aminolevulinate	MS Level 2
HMDB00042	Acetate	MS Level 1
HMDB00060	Acetoacetate	MS Level 2
HMDB00094	Citrate	MS Level 1
HMDB00064	Creatine	MS Level 1
HMDB00562	Creatinine	MS Level 1
HMDB00112	D-Glucose	MS Level 1
HMDB00108	Ethanol	MS Level 1
HMDB00142	Formate	MS Level 2
HMDB00663	Glucarate	MS Level 2
HMDB00131	Glycerol	MS Level 1
HMDB00123	Glycine	MS Level 1
HMDB00128	Guanidoacetate	MS Level 2
HMDB00190	Lactate	MS Level 1
HMDB00161	L-Alanine	MS Level 1
HMDB00062	L-Carnitine	MS Level 2
HMDB00641	L-Glutamine	MS Level 1
HMDB00177	L-Histidine	MS Level 1
HMDB00687	L-Leucine	MS Level 1
HMDB00159	L-Phenylalanine	MS Level 1
HMDB00167	L-Threonine	MS Level 2
HMDB00158	L-Tyrosine	MS Level 1

Database identifier	Metabolite Identification	Reliability
HMDB00883	L-Valine	MS Level 1
HMDB00243	Pyruvate	MS Level 1

MS = metabolomics standard

Figure legends

Fig 1: T1 (left) and T2-weighted (right) MRI images demonstrating POD scores of 2 (moderate sclerosis) and 3* (SCB resorption with bone marrow involvement) in the lateral and medial condyles respectively. Lateral is to the left of the image.

Fig 2: Frontal STIR MRI image demonstrating a POD lesion with increased fluid signal in the lateral condyle. Lateral is to the left of the image.

Fig 3: Unsupervised PCA scores plot of POD (green) and control (red) samples demonstrating minimal variance between groups. Shading represents 95% confidence region.

Fig 4: Supervised PLS-DA scores plot showing POD and control groups with the two components demonstrating best fit of the model ($R^2 = 0.67$, $Q^2 = 0.34$).

Fig 5: VIP scores for the 25 most influential buckets of PLS-DA decreased levels of glucose and lactate in the POD group were not statistically significant between groups.

Supporting Information

Supplementary Item 1: Lesion grading using the POD scoring system adapted from Olive *et al*. [23]

References

[1] Barr, E.D., Pinchbeck, G.L., Clegg, P.D., Boyde, A. and Riggs, C.M. (2009) Post mortem evaluation of palmar osteochondral disease (traumatic osteochondrosis) of the metacarpo/metatarsophalangeal joint in Thoroughbred racehorses. *Equine Vet. J.* **41**, 366-371.

[2] Powell, S.E. (2012) Low-field standing magnetic resonance imaging findings of the metacarpo/metatarsophalangeal joint of racing Thoroughbreds with lameness localised to the region: a retrospective study of 131 horses. *Equine Vet. J.* **44**, 169-177.

[3] Pinchbeck, G.L., Clegg, P.D., Boyde, A. and Riggs, C.M. (2013) Pathological and clinical features associated with palmar/plantar osteochondral disease of the metacarpo/metatarsophalangeal joint in Thoroughbred racehorses. *Equine Vet. J.* **45**, 587-592.

[4] Bani Hassan, E., Mirams, M., Mackie, E.J. and Whitton, R.C. (2017) Prevalence of subchondral bone pathological changes in the distal metacarpi/metatarsi of racing Thoroughbred horses. *Aust. Vet. J.* **95**, 362-369.

[5] Easton, K.L. and Kawcak, C.E. (2007) Evaluation of increased subchondral bone density in areas of contact in the metacarpophalangeal joint during joint loading in horses. *Am. J. Vet. Res.* **68**, 816-821.

[6] Murray, R.C., Branch, M.V., Tranquille, C. and Woods, S. (2005) Validation of magnetic resonance imaging for measurement of equine articular cartilage and subchondral bone thickness. *Am. J. Vet. Res.* **66**, 1999-2005.

[7] Dyson, S.J. and Murray, R. (2007) Magnetic Resonance Imaging of the Equine Fetlock. *Clin. Tech. Equine Prac.* **6**, 62-77.

[8] Sherlock, C.E., Mair, T.S. and Ter Braake, F. (2009) Osseous lesions in the metacarpo(tarso)phalangeal joint diagnosed using low-field magnetic resonance imaging in standing horses. *Vet. Radiol. Ultrasound* **50**, 13-20.

[9] Olive, J., d'Anjou, M.A., Alexander, K., Beauchamp, G. and Theoret, C.L. (2010) Correlation of signal attenuation-based quantitative magnetic resonance imaging with quantitative computed

tomographic measurements of subchondral bone mineral density in metacarpophalangeal joints of horses. *Am. J. Vet. Res.* **71**, 412-420.

[10] Olive, J., D'Anjou, M.A., Alexander, K., Laverty, S. and Theoret, C. (2010) Comparison of magnetic resonance imaging, computed tomography, and radiography for assessment of noncartilaginous changes in equine metacarpophalangeal osteoarthritis. *Vet. Radiol. Ultrasound* **51**, 267-279.

[11] Escalona, E.E., Leng, J., Dona, A.C., Merrifield, C.A., Holmes, E., Proudman, C.J. and Swann, J.R. (2015) Dominant components of the Thoroughbred metabolome characterised by (1) H-nuclear magnetic resonance spectroscopy: A metabolite atlas of common biofluids. *Equine Vet. J.* **47**, 721-730.

[12] Goodacre, R., Vaidyanathan, S., Dunn, W.B., Harrigan, G.G. and Kell, D.B. (2004) Metabolomics by numbers: acquiring and understanding global metabolite data. *Trends Biotechnol.* **22**, 245-252.

[13] McIlwraith, C.W., Kawcak, C.E., Frisbie, D.D., Little, C.B., Clegg, P.D., Peffers, M.J., Karsdal, M.A., Ekman, S., Laverty, S., Slayden, R.A., Sandell, L.J., Lohmander, L.S. and Kraus, V.B. (2018) Biomarkers for equine joint injury and osteoarthritis. *J. Orthop. Res.* **36**, 823-831.

[14] Zheng, K., Shen, N., Chen, H., Ni, S., Zhang, T., Hu, M., Wang, J., Sun, L. and Yang, X. (2017) Global and targeted metabolomics of synovial fluid discovers special osteoarthritis metabolites. *J. Orthop. Res.* **35**, 1973-1981.

[15] Hugle, T., Kovacs, H., Heijnen, I.A., Daikeler, T., Baisch, U., Hicks, J.M. and Valderrabano, V. (2012) Synovial fluid metabolomics in different forms of arthritis assessed by nuclear magnetic resonance spectroscopy. *Clin. Exp. Rheumatol.* **30**, 240-250.

[16] Priori, R., Scrivo, R., Brandt, J., Valerio, M., Casadei, L., Valesini, G. and Manetti, C. (2013) Metabolomics in rheumatic diseases: the potential of an emerging methodology for improved patient diagnosis, prognosis, and treatment efficacy. *Autoimmun. Rev.* **12**, 1022-1030.

[17] Hsueh, M.F., Onnerfjord, P. and Kraus, V.B. (2014) Biomarkers and proteomic analysis of osteoarthritis. *Matrix Biol.* **39**, 56-66.

[18] Mickiewicz, B., Kelly, J.J., Ludwig, T.E., Weljie, A.M., Wiley, J.P., Schmidt, T.A. and Vogel, H.J. (2015) Metabolic analysis of knee synovial fluid as a potential diagnostic approach for osteoarthritis. *J. Orthop. Res.* **33**, 1631-1638.

[19] Anderson, J.R., Chokesuwattanaskul, S., Phelan, M.M., Welting, T., Lian, L. Y. Peffers, M.J. and Wright, H. (2018) 1H NMR metabolomics identifies underlying inflammatory pathology in osteoarthritis and rheumatoid arthritis synovial joints. *J. Proteom. Res.* **17**, 3780-3790.

[20] Anderson, J.R., Phelan, M.M., Clegg, P.D., Peffers, M.J. and Rubio-Martinez, L.M. (2018) Synovial Fluid Metabolites Differentiate between Septic and Nonseptic Joint Pathologies. *J. Proteome Res.* **17**, 2735-2743.

[21] Lacitignola, L., Fanizzi, F.P., Francioso, E. and Crovace, A. (2008) 1H NMR investigation of normal and osteo-arthritic synovial fluid in the horse. *Vet. Comp. Orthop. Traumatol.* **21**, 85-88.

[22] Desjardin, C., Riviere, J., Vaiman, A., Morgenthaler, C., Diribarne, M., Zivy, M., Robert, C., Le Moyec, L., Wimel, L., Lepage, O., Jacques, C., Cribiu, E. and Schibler, L. (2014) Omics technologies provide new insights into the molecular physiopathology of equine osteochondrosis. *BMC Genomics* **15**, 947.

[23] Olive, J., Serraud, N., Vila, T. and Germain, J.P. (2017) Metacarpophalangeal joint injury patterns on magnetic resonance imaging: A comparison in racing Standardbreds and Thoroughbreds. *Vet. Radiol. Ultrasound* **58**, 588-597.

[24] Sumner, L.W., Amberg, A., Barrett, D., Beale, M.H., Beger, R., Daykin, C.A., Fan, T.W.M., Fiehn, O., Goodacre, R., Griffin, J.L., Hankemeier, T., Hardy, N., Harnly, J., Higashi, R., Kopka, J., Lane, A.N., Lindon, J.C., Marriott, P., Nicholls, A.W., Reily, M.D., Thaden, J.J. and Viant, M.R. (2007) Proposed minimum reporting standards for chemical analysis Chemical Analysis Working Group Metabolomics Standards Initiative. *Metabolomics* **3**, 211-221.

[25] Yang, G., Zhang, H., Chen, T., Zhu, W., Ding, S., Xu, K., Xu, Z., Guo, Y. and Zhang, J. (2016) Metabolic analysis of osteoarthritis subchondral bone based on UPLC/Q-TOF-MS. *Anal. Bioanal. Chem.* **408**, 4275-4286.

[26] Sokolove, J. and Lepus, C.M. (2013) Role of inflammation in the pathogenesis of osteoarthritis: latest findings and interpretations. *Ther. Adv. Musculoskelet. Dis.* **5**, 77-94.

[27] Mobasheri, A., Rayman, M.P., Gualillo, O., Sellam, J., van der Kraan, P. and Fearon, U. (2017) The role of metabolism in the pathogenesis of osteoarthritis. *Nat. Rev. Rheumatol.* **13**, 302-311.

[28] Peansukmanee, S, Vaughan-Thomas, A., Carter, S.D., Clegg, P.D., Taylor, S., Redmond, C. and Mobasheri, A. (2009) Effects of hypoxia on glucose transport in primary equine chondrocytes in vitro and evidence of reduced GLUT1 gene expression in pathologic cartilage in vivo. *J. Orthop. Res.* **27**, 529-535.

[29] Lotz, M. and Loeser, R.F. (2012) Effects of ageing on articular cartilage homeostasis. *Bone* **51**, 241-248.

[30] Markley, J.L., Bruschweiler, R., Edison, A.S., Eghbalnia, H.R., Powers, R., Raftery, D. and Wishart, D.S. (2017) The future of NMR-based metabolomics. *Curr. Opin. Biotechnol.* **43**, 34-40.

[31] Soininen, P., Kangas, A.J., Wurtz, P., Tukiainen, T., Tynkkynen, T., Laatikainen, R., Jarvelin, M.R., Kahonen, M., Lehtimaki, T., Viikari, J., Raitakari, O.T., Savolainen, M.J. and Ala-Korpela, M. (2009) High-throughput serum NMR metabonomics for cost-effective holistic studies on systemic metabolism. *Analyst.* **134**, 1781-1785.

[32] Merrifield, C.A., Lewis, M., Claus, S.P., Beckonert, O.P., Dumas, M.E., Duncker, S., Kochhar, S., Rezzi, S., Lindon, J.C., Bailey, M., Holmes, E. and Nicholson, J.K. (2011) A metabolic system-wide characterisation of the pig: a model for human physiology. *Mol. Biosyst.* **7**, 2577-2588.

[33] Davis, A.M., Fan, X., Shen, L., Robinson, P. and Riggs, C.M. (2017) Improved radiological diagnosis of palmar osteochondral disease in the Thoroughbred racehorse. *Equine Vet. J.* **49**, 454-460.

[34] Pinto, J., Domingues, M.R.M., Galhano, E., Pita, C., Almeida, M.d.C., Carreira, I.M. and Gil, A.M. (2014) Human plasma stability during handling and storage: impact on NMR metabolomics. *Analyst.* **139**, 1168-1177.

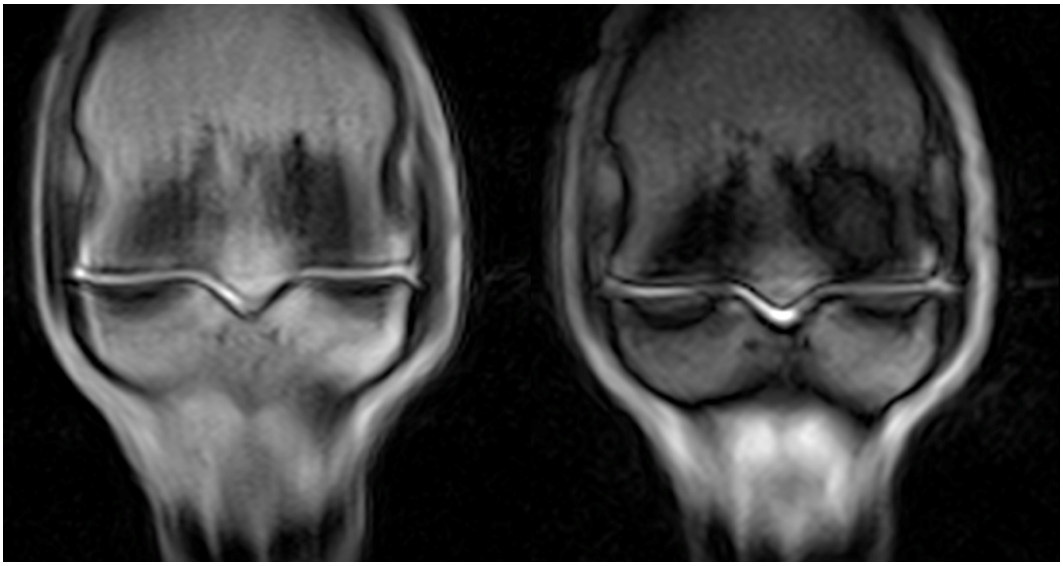

evj_13199_f1.tif

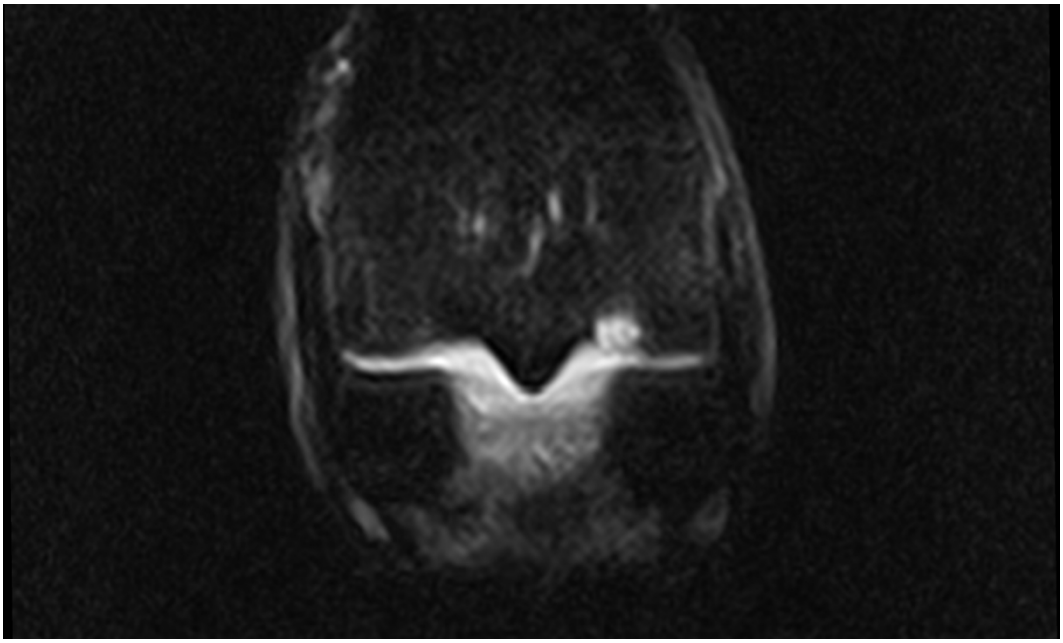

evj_13199_f2.tif

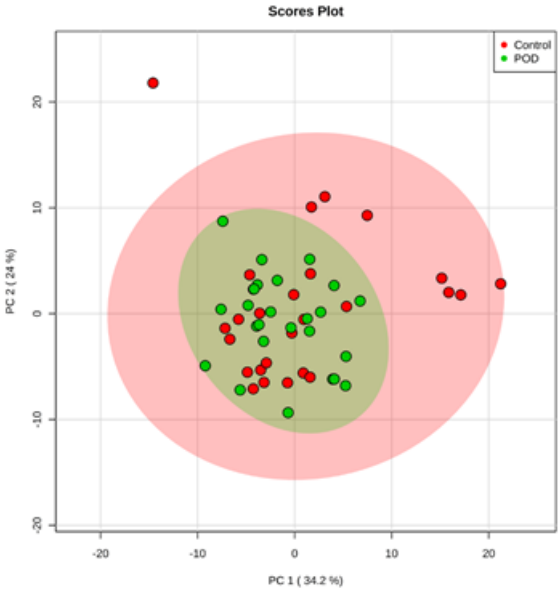

evj_13199_f3.tif

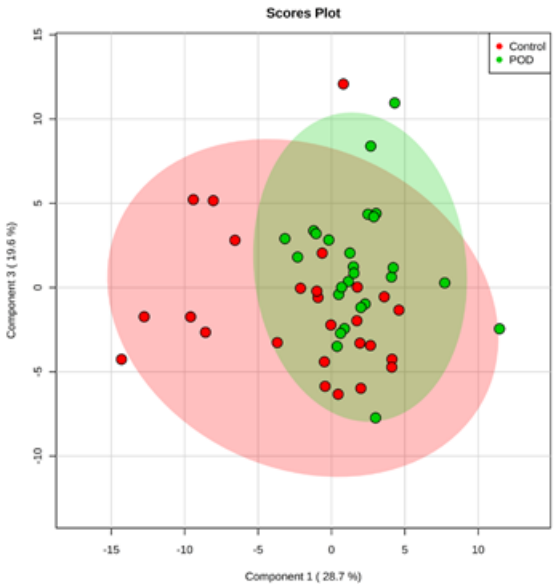

evj_13199_f4.tif

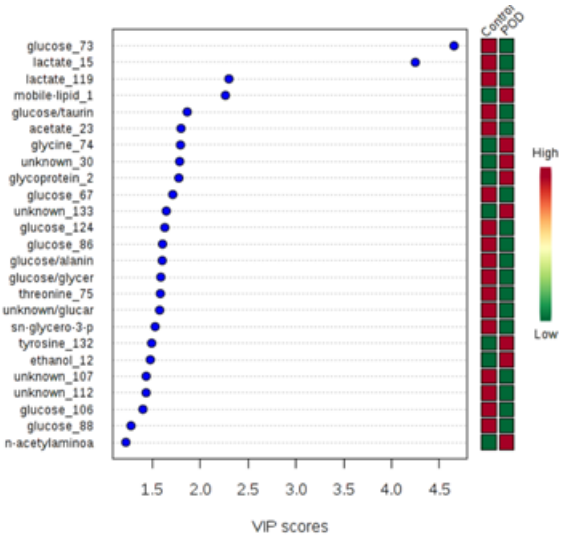

evj_13199_f5.tif